Strain distribution in bent ZnO microwires

C. P. Dietrich, M. Lange, F. J. Klüpfel, H. von Wenckstern, R. Schmidt-Grund et al.

Citation: Appl. Phys. Lett. **98**, 031105 (2011); doi: 10.1063/1.3544939
View online: http://dx.doi.org/10.1063/1.3544939
View Table of Contents: http://apl.aip.org/resource/1/APPLAB/v98/i3
Published by the American Institute of Physics.

Strain distribution in bent ZnO microwires

C. P. Dietrich,[a] M. Lange, F. J. Klüpfel, H. von Wenckstern, R. Schmidt-Grund, and M. Grundmann
Institut für Experimentelle Physik II, Universität Leipzig, Linnéstr. 5, 04103 Leipzig, Germany

(Received 23 November 2010; accepted 3 January 2011; published online 20 January 2011)

ZnO microwires grown by carbothermal reduction were mechanically bent and the uniaxial stress state was studied with spatially resolved low-temperature photoluminescence. Inhomogeneous (tensile and compressive) stress (up to ±1 GPa) is visualized by the redshift and blueshift of the wire luminescence. Experimentally determined tensile and compressive strain along the *c*-axis (wire axis) of up to 1.5 %, symmetrically distributed with respect to the central axis (neutral fiber), is achieved, resulting in maximum energetic shifts of ±30 meV. Within these experiments, we are able to precisely determine the direct relation between energetic shift of the free A-exciton energy and strain to (-2.04 ± 0.02) eV. © *2011 American Institute of Physics*. [doi:10.1063/1.3544939]

Semiconductor nanostructures and microstructures are attracting more and more interest on the pathway toward nanoscale and microscale technologies.[1,2] The rising complexity of modern devices is based on the usage of semiconductor heterostructures that underlie various strain effects due to lattice mismatch.[3] Thus, strain engineering has become an important field in device design.[4,5] Especially, advanced transistors benefit from the enhanced mobility in strained silicon.[6] Also, carbon nanotubes are known to react very sensitively to deformations and show different electrical and magnetic properties under strain.[7] Besides these materials, the wide-band gap semiconductor ZnO has outstanding optical[8] and piezoelectrical properties[9] that can be carefully modified under tensile or compressive strain.[10–12] ZnO is a perfect material for the fabrication of strain generators[13] and piezoelectric sensors.[14,15] However, the exact deformation parameters relating strain and electronic structure in semiconductors are still uncertain for ZnO. Only a few experimental publications exist where deformation potentials for ZnO (Ref. 16–19) are reported.

In this letter, we demonstrate and evaluate the uniaxial stress effect on the band edge of ZnO microwires and present a simple experiment that enables the precise determination of the deformation potential of type $\partial E_A / \partial \varepsilon_c$. Therein, we achieve energetic shifts of the wire luminescence up to ±30 meV for strain $\varepsilon_c = \pm 1.5\%$ along the *c*-axis (wire axis), respectively. We note that this is a rather large strain, larger than the values reported up to now for ZnO (Ref. 16) under uniaxial (compressive) stress and that in SiGe nanoscrolls built-in by lattice-mismatched heteroepitaxy.[20,21] The outer part of the wire offers the unique opportunity to study material under large tensile stress, which is impossible to reach with conventional high-pressure experiments.

All investigated ZnO microwires were grown by carbothermal vapor-phase transport.[22] ZnO (5N purity) and carbon (4N purity) powders were mixed and pressed to form a tablet and then put into a tube furnace system. The system was heated up to 1150 °C (the temperature at which ZnO and C have similar Gibb's free energies and C atoms are able to reduce ZnO to vapor zinc and oxygen). The growth process was performed at ambient air conditions for optimal reoxidation into solid ZnO microwires. The so-formed wires have diameters of 0.4–50 μm and lengths of 0.1–20 mm. Furthermore, they show perfectly shaped hexagonal cross sections, indicating the *c*-axis to be parallel to the wire axis. The diameters of the microwires were measured by means of scanning electron microscopy within an accuracy of 0.01 μm.

The photoluminescence (PL) measurements were performed in a micro-PL setup. The microwires were excited by the 325 nm line of a HeCd laser focused to a minimum spot size of 1 μm by an objective with 4 mm focal distance and a numerical aperture of 0.42. The emitted light is spectrally dispersed by a monochromator with 32 cm focal length and a 2400 groves/mm UV-blazed grating (minimum spectral bandwidth is 0.06 nm corresponding to 0.6 meV at ZnO band edge emission) and detected by a nitrogen-cooled, back-illuminated charge-coupled device. All spectra were recorded at $T = 15$ K from microwires in a helium flow cryostat.

In order to precisely investigate the effect of tensile and compressive strain along the wire, low-temperature PL spectra of all ZnO microwires were recorded prior to the bending. Glass substrates served as base for the wires, which were then mechanically bent with tweezers. Due to adhesion forces between the bent microwires and the glass substrates, the wires remained bent without additional fixation and associated additional strain (Fig. 1).

The shape of the microwires under bending was carefully checked to classify the kind of strain induced into the wires. All wires showed a constant diameter (±1%) over several hundreds of microns (much larger than the laser spot). Further, atomic force microscopy (AFM) measure-

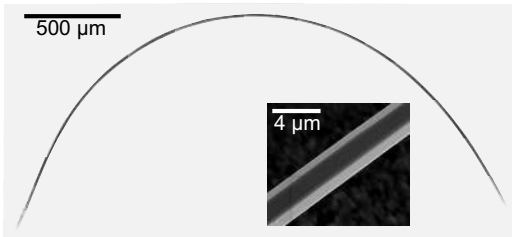

FIG. 1. Composed optical microscopic image of a bent ZnO microwire with diameter $d = 8.5$ μm. The minimum radius of curvature R_C is 700 μm. Inset, top view: SEM image of a bent ZnO microwire with $d = 3.1$ μm.

[a]Electronic mail: c.dietrich@physik.uni-leipzig.de.

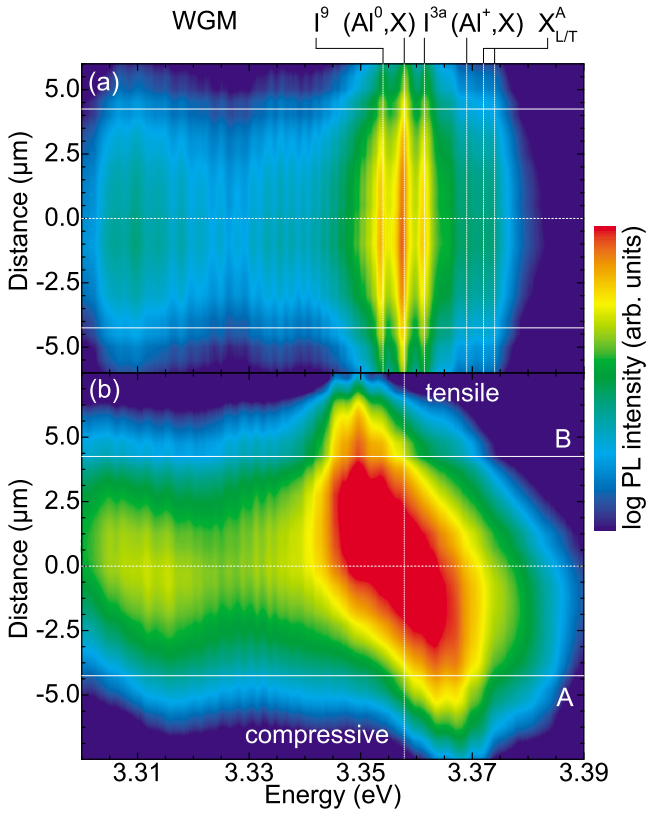

FIG. 2. (Color online) Low-temperature ($T=15$ K) PL line scans of a ZnO microwire with $d=8.5$ μm (a) before and (b) after bending, respectively. The center of the wire (neutral fiber) is set as zero for the position axis. The most prominent recombination peaks (indicated by vertical dotted lines) as well as appearing WGMs are labeled for the unbent microwire. The edges of the microwire are highlighted by solid lines.

ments (not shown here) revealed that the top facet of all microwires was parallel to the surface of the glass substrate (no tilt or twist). Therefore, we consequently assume a stress that is uniaxial along the c-axis.

The maximum amount of tensile and compressive strain ε_c that is induced into the wire by bending depends on the diameter d of the respective wire and the radius of curvature R_C and can be calculated as[11]

$$\varepsilon_c^{\max} = \frac{c - c_0}{c_0} = \pm \frac{d}{2R_C}, \tag{1}$$

with c and c_0 being the lattice constants at the outer and inner surface of the wire in the strained and unstrained case, respectively. The local radius of curvature R_C was calculated from the bending along the whole length of the wires within 1 μm accuracy. Shear strains are of the order c_0/R_C and are neglected.

A typical low-temperature PL line scan across an unbent ZnO microwire with a diameter of $d=8.51$ μm can be seen in Fig. 2(a). The microwire luminescence shows prominent transitions of neutral (3.3580 eV, I_6 line) and ionized (3.3691 eV, I_0 line) aluminum-bound (Al^0,X) and (Al^+,X), as well as longitudinal (transversal) free excitons at 3.3718 eV (3.3738 eV) indicated by vertical dotted lines. The full width at half maximum (FWHM) of 0.3 meV of the (Al^0,X) peak indicates high material quality (measured in a slightly modified PL setup with a 1 m focal length monochromator providing minimum spectral bandwidth of 0.1 meV). Moreover, below 3.355 eV, the spectrum is modulated by several peaks with decreasing spectral distance. These peaks can be assigned to whispering gallery modes (WGMs) that arise in well-shaped hexagonal structures.[23] The WGMs in our wires have complete photonic character and form inside a closed roundtrip due to constructive interference of the light beam enabled by the total internal reflection at the side facets of the hexagon. All investigated unbent ZnO microwires exhibited PL spectra similar to that of Fig. 2(a).

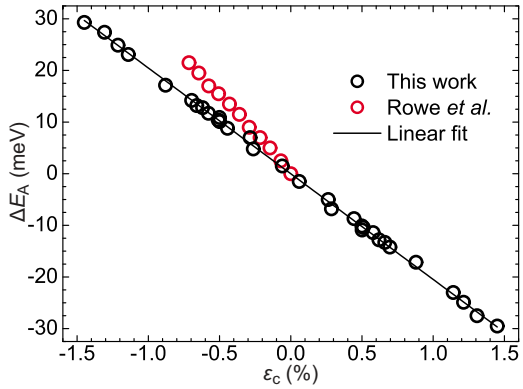

FIG. 3. (Color online) Shift ΔE of free A-exciton emission energy E_A vs strain at low temperatures ($T=15$ K). The solid line represents a linear least-squares fit to the experimental data from six microwires with a slope of $\partial E_A/\partial \varepsilon_c = (-2.04 \pm 0.02)$ eV. Error bars are smaller than the symbol size. Values from Rowe *et al.* (Ref. 16) recalculated for $E_A(\varepsilon_c)$ according to Eq. (2) and elastic constants from Ref. 25 are given for comparison as red circles.

The spectral line scan across the same ZnO microwire after bending at a local position with $R_C=958$ μm can be seen in Fig. 2(b). The step width was set to 500 nm to be aware of exciton diffusion, since excitons have typical diffusion lengths of about 200 nm and therefore limit the resolution of such a line scan. The facet edges of the wire are indicated by horizontal dashed lines. At position A, the dominant recombination process is considerably blueshifted due to compressive strain, whereas the main luminescence is redshifted at position B due to tensile strain. By crossing the wire (from A to B), the (Al^0,X) peak position shifts linearly from 3.3668 to 3.3493 eV ($\Delta E=17.5$ meV), passing the vertical dotted line in the center of the wire. This indicates that the central axis represents the neutral fiber as expected. Accordingly, we conclude for a symmetric distribution of compressive and tensile strain inside the wires. Note that the energy of the WGM does not depend on the local position since it is an *integral* property of the wire cross section.

Further, in agreement with the (Al^0,X) transition, the free exciton emission shifts from 3.3648 to 3.3825 eV ($\Delta E=17.7$ meV). Thus, the localization energy of bound excitons can be assumed to be strain-independent. The FWHM of the near-band edge emission is obviously increased tremendously at the neutral fiber due to insufficient spatial resolution. We note that at the outer parts of the wires, the fine structure of the near-band edge recombination spectrum is well resolved and thus the maximum energetic shift can be precisely determined

The energetic shift of the free A-exciton emission versus strain is depicted in Fig. 3. Spatially resolved data from six microwires with different d and R_C are combined. A linear fit to the experimental data yields $\partial E_A/\partial \varepsilon_c = (-2.04 \pm 0.02)$ eV, taking into account the errors for diam-

eters, radii, and energetic shifts. There is no experimental evidence for a nonlinearity in the dependence $\Delta E_A(\varepsilon_c)$.

No reports have been published up to now that present the evaluation of the uniaxial strain effect in ZnO wires. Han *et al.*[10] as well as Xue *et al.*[11] performed cathodoluminescence measurements on mechanically bent ZnO nanowires. Han *et al.* only observed a redshift and broadening for nanowires ($d=0.15$ μm). Xue *et al.* report blueshifted and redshifted wire luminescence due to compressive and tensile strain and deduce $\partial E_A/\partial\varepsilon_c=-0.37$ eV, a value much smaller than the one evaluated here from our data. We attribute this to the lack of sufficient spatial resolution of cathodoluminescence (5 kV, 10^5 pA) in Ref. 11 to determine the local exciton recombination energy in the outer parts of the nanowire ($d=0.125$ μm).

Probing the uniaxial stress effect by an externally applied homogeneous stress as done by Rowe *et al.*[16] is limited to compressive deformation. Tensile stress is not accessible since pulling forces cannot be accomplished. Tensile ε_c can only be achieved in strained epitaxial layers, but the strain values therein are limited to a few tenths of a percent.[24] In contrast to that, we achieved tensile *and* compressive strain, symmetrically distributed with respect to the central axis of the wire, exceeding values reported in Ref. 16. The experimental data from Rowe *et al.* are given for comparison in Fig. 3 using the elastic constants from Ref. 25 and the formula

$$\varepsilon_{zz}=\frac{C_{11}+C_{12}}{(C_{11}+C_{12})C_{33}-2C_{13}^2}\sigma_{zz}=S_{33}\sigma_{zz}, \tag{2}$$

with C_{ij} being the elastic constants and S_{ij} being the stiffness coefficients ($S_{33}=6.94\times10^{-13}$ cm^2/dyn). They found a nonlinear relation between energetic shift and applied stress for stress values above 8×10^9 dyn/cm^2(=0.8 GPa). Our data suggest that the observed nonlinearity is not due to a nonlinearity of the strain regime, but rather due to the nonlinearity of the stress-strain relation. We note that from pressure experiments, only $\partial E/\partial\sigma$ can be extracted, whereas our measurements provide the direct determination of $\partial E/\partial\varepsilon$.

Recently, nanostructures gained more and more attention in fields of material science and physics. Consequently, one needs to consider transferring the experiment to the nanoscale. Desai and Haque[26] found out that the fracture strain of nanowires is increased when decreasing the wire diameter. This allows the application of very large stresses to nanoscale wires. As a consequence, the tensile strained part of a bent nanowire should be much larger than the compressive strained part due to repulsion forces between atoms. Nevertheless, theory predicts a phase transition from direct to indirect band gap when applying even higher compressive stresses to ZnO nanowires.[12] Note that spatially resolved luminescence experiments on nanowires have insufficient resolution. For this case, spatially integrated spectra need to be evoluted.

In conclusion, we experimentally evoked and evaluated the uniaxial stress effect in ZnO microwires grown by carbothermal reduction. We were able to mechanically bend the wires to minimum radii of curvature of 400 μm and respective maximum *c*-axis strain of about $\pm1.5\%$. Line scans perpendicular to the wire axis showed maximum energetic shifts of the dominant excitonic recombination peaks of ±30 meV. The compressive and tensile strain inside the wires turned out to be symmetrically distributed perpendicular to the wire axis. For uniaxial stress, we determined the direct relation between energetic shift of the free A-exciton emission energy and strain to $\partial E_A/\partial\varepsilon_c=(-2.04\pm0.02)$ eV. We emphasize that within our experiments, it is possible to study large tensile stress in materials which is otherwise not accessible. This possibility opens up the door for new physics.

This work has been supported by Leipzig School of Natural Sciences BuildMoNa (Grant No. GS 185/1) and the European Social Fund (ESF) within Nachwuchsforschergruppe "Multiscale functional structures." We gratefully acknowledge preparation of ZnO-carbon targets by G. Ramm and AFM measurements by T. Böntgen.

[1] M. S. Gudiksen, L. J. Lauhon, J. F. Wang, D. C. Smith, and C. M. Lieber, Nature (London) **415**, 617 (2002).
[2] M. H. Huang, S. Mao, H. Feick, H. Yan, Y. Wu, H. Kind, E. Weber, R. Russo, and P. Yang, Science **292**, 1897 (2001).
[3] M. Asif Khan, J. W. Yang, G. Simin, R. Gaska, M. S. Shur, H.-C. zur Loye, G. Tamulaitis, A. Zukauskas, D. J. Smith, D. Chandrasekhar, and R. Bicknell-Tassius, Appl. Phys. Lett. **76**, 1161 (2000).
[4] M. Ieong, B. Doris, J. Kedzierski, K. Rim, and M. Yang, Science **306**, 2057 (2004).
[5] R. R. He and P. D. Yang, Nat. Nanotechnol. **1**, 42 (2006).
[6] M. V. Fischetti, F. Gámiz, and W. Hänsch, J. Appl. Phys. **92**, 7320 (2002).
[7] T. W. Tombler, C. Zhou, L. Alexseyev, J. Kong, H. Dai, L. Liu, C. S. Jayanthi, M. Tang, and S. Y. Wu, Nature (London) **405**, 769 (2000).
[8] C. Czekalla, C. Sturm, R. Schmidt-Grund, B. Q. Cao, M. Lorenz, and M. Grundmann, Appl. Phys. Lett. **92**, 241102 (2008).
[9] C. Klingshirn, Phys. Status Solidi B **244**, 3027 (2007).
[10] X. Han, L. Kou, X. Lang, J. Xia, N. Wang, R. Qin, J. Lu, J. Xu, Z. Liao, X. Zhang, X. Shan, X. Song, J. Gao, W. Guo, and D. Yu, Adv. Mater. **21**, 4937 (2009).
[11] H. Xue, N. Pan, M. Li, Y. Wu, X. Wang, and J. G. Hou, Nanotechnology **21**, 215701 (2010).
[12] S.-C. Ling, T.-C. Lu, S.-P. Chang, J.-R. Chen, H.-C. Kuo, and S.-C. Wang, Appl. Phys. Lett. **96**, 231101 (2010).
[13] X. Wang, J. Song, J. Liu, and Z. L. Wang, Science **316**, 102 (2007).
[14] J. Zhou, Y. Gu, P. Fei, W. Mai, Y. Gao, R. Yang, G. Bao, and Z. L. Wang, Nano Lett. **8**, 3035 (2008).
[15] K. Sun, H. Zhang, L. Hu, D. Yu, S. Qiao, J. Sun, J. Bian, X. Chen, L. Zhang, Q. Fu, and Z. Zhao, Phys. Status Solidi A **207**, 488 (2010).
[16] J. E. Rowe, M. Cardona, and F. H. Pollak, Solid State Commun. **6**, 239 (1968); **7**, 8 (1969).
[17] D. W. Langer, R. N. Euwema, K. Era, and T. Koda, Phys. Rev. B **2**, 4005 (1970).
[18] J. Wrzesinski and D. Fröhlich, Phys. Rev. B **56**, 13087 (1997).
[19] W. Shan, W. Walukiewicz, J. W. Ager III, K. M. Yu, Y. Zhang, S. S. Mao, R. Kling, C. Kirchner, and A. Waag, Appl. Phys. Lett. **86**, 153117 (2005).
[20] O. G. Schmidt and N. Y. Jin-Phillipp, Appl. Phys. Lett. **78**, 3310 (2001).
[21] M. Grundmann, Appl. Phys. Lett. **83**, 2444 (2003).
[22] M. Lorenz, A. Rahm, B. Cao, J. Zúñiga-Pérez, E. M. Kaidashev, N. Zhakarov, G. Wagner, T. Nobis, C. Czekalla, G. Zimmermann, and M. Grundmann, Phys. Status Solidi B **247**, 1265 (2010).
[23] T. Nobis, E. M. Kaidashev, A. Rahm, M. Lorenz, and M. Grundmann, Phys. Rev. Lett. **93**, 103903 (2004).
[24] T. Makino, T. Yasuda, Y. Segawa, A. Ohtomo, K. Tamura, M. Kawasaki, and H. Koinuma, Appl. Phys. Lett. **79**, 1282 (2001).
[25] T. B. Bateman, J. Appl. Phys. **33**, 3309 (1962).
[26] A. V. Desai and M. A. Haque, Sens. Actuators, A **134**, 169 (2007).